

# Synthesis, Structure, and Magnetic Properties of $[\text{Mn}^{\text{III}}(\text{salpn})\text{NCS}]_n$ , a Helical Polymer, and the Dimer $[\text{Mn}^{\text{III}}(\text{salpn})\text{NCS}]_2$ . Weak Ferromagnetism in $[\text{Mn}^{\text{III}}(\text{salpn})\text{NCS}]_n$ Related to the Strong Magnetic Anisotropy in Jahn–Teller Mn(III) ( $\text{salpnH}_2 = N,N'$ -Bis(salicylidene)-1,3-diaminopropane)

S. Sailaja,<sup>†</sup> K. Rajender Reddy,<sup>†</sup> M. V. Rajasekharan,<sup>\*,†</sup> C. Hureau,<sup>‡</sup> E. Rivière,<sup>‡</sup> J. Cano,<sup>‡</sup> and J.-J. Girerd<sup>\*,‡</sup>

School of Chemistry, University of Hyderabad, Hyderabad 500 046, India, and Laboratoire de Chimie Inorganique, UMR CNRS 8613, Institut de Chimie Moléculaire d'Orsay, Université Paris-Sud, 91405 Orsay Cedex, France

Received April 18, 2002

Dimeric  $[\text{Mn}(\text{salpn})\text{NCS}]_2$  (**1**) and polymeric  $[\text{Mn}(\text{salpn})\text{NCS}]_n$  (**2**) are formed by the reaction of  $\text{Mn}(\text{CH}_3\text{CO}_2)_2 \cdot 4\text{H}_2\text{O}$ , the schiff base, and thiocyanate. The formation of the two polymorphic forms is solvent and temperature dependent. **1**: orthorhombic, space group *Pbca*, with  $a = 12.573(2)$  Å,  $b = 13.970(7)$  Å,  $c = 18.891(9)$  Å, and  $Z = 8$ . **2**: orthorhombic, space group *Pna*<sub>21</sub>, with  $a = 12.5277(14)$  Å,  $b = 11.576(2)$  Å,  $c = 11.513(2)$  Å, and  $Z = 4$ . The dimers in **1** are held together by weak noncovalent  $\text{S} \cdots \pi$  (phenyl) interactions leading to a chain along the *a*-axis. Each monomeric unit of the polymer in **2** is related to its adjacent ones by a 2-fold screw axis leading to a helix along the *c*-axis. The exchange coupling is nondetectable in the dimer. The magnetic susceptibility of the helical chain fits a classical chain law with  $J = -3.2 \text{ cm}^{-1}$  and shows a weak ferromagnetic ordering below 7 K due to spin canting effects.

## Introduction

The combination of a pseudohalide ion and a tetradentate Schiff base (SB) ligand is suitable for making neutral M(III) complexes of the type  $\text{M}(\text{SB})\text{X}$ . The structure and magnetic properties of  $\text{Mn}(\text{salpn})\text{N}_3$  and  $\text{Fe}(\text{salpn})\text{N}_3$  have been previously published,<sup>1</sup> where the relevant literature on similar Mn(III) complexes has been reviewed. The manganese complex has a helical polymeric structure with a 1,3-azide bridge, while the iron analogue has a dimeric structure having cis-octahedrally coordinated salpn and a 1,1-azide bridge. It is now shown that the analogous thiocyanate complex of manganese can be obtained in two forms, depending upon the solvent and crystallization temperature. One polymorph is dimeric, having unsymmetrical phenolate bridges and

terminal N-bonded thiocyanate ligands. The second one is similar to the azide complex in having a helical polymeric structure.

A compound having the same empirical formula as the present one as well as a hydrate has been previously prepared<sup>2,3</sup> but not structurally characterized. Further, the catalytic efficiency of this compound toward epoxidation of alkenes has been investigated.<sup>4</sup> The analogous complex of salen,  $\text{Mn}(\text{salen})\text{NCS}$ , the magnetic properties of which were reported by Kennedy and Murray,<sup>5</sup> has a monomeric five-coordinate structure<sup>6</sup> with weak axial perturbation by neighboring phenolate oxygen ( $\text{salenH}_2 = N,N'$ -bis(salicylidene)-1,2-diaminoethane). Several such dimeric complexes showing ferromagnetic as well as antiferromagnetic coupling are now

\* To whom correspondence should be addressed. E-mail: mvrsc@uohyd.ernet.in (M.V.R.); jjgirerd@icmo.u-psud.fr (J.-J.G.).

<sup>†</sup> University of Hyderabad.

<sup>‡</sup> Université Paris-Sud.

(1) Reddy, K. R.; Rajasekharan, M. V.; Tuchagues, J.-P. *Inorg. Chem.* **1998**, *37*, 5978.

(2) Kolawole, G. A. *Synth. React. Inorg. Met.-Org. Chem.* **1993**, *23*, 907.

(3) Ashmawy, F. M.; McAuliffe, C. A.; Parish, R. V.; Tames, J. *Inorg. Chim. Acta* **1985**, *103*, 133.

(4) Agarwal, D. D.; Bhatnagar, R. P.; Jain, R.; Srivastava, S. *J. Chem. Soc., Perkin Trans. 2* **1990**, 989.

(5) Kennedy, B. J.; Murray, K. S. *Inorg. Chem.* **1985**, *24*, 1552.

(6) Mikuriya, M.; Yamato, Y.; Tokii, T. *Bull. Chem. Soc. Jpn.* **1992**, *65*, 1466.

known and the metric parameters of the phenolate bridge and the exchange parameters have been reviewed in a recent paper by Miyasaka et al.<sup>7</sup> Crystallographic characterizations of chain compounds of Mn(III) having pseudohalide bridges are relatively rare.<sup>1,8–10</sup> These compounds generally show a magnetic phase transition at low temperatures.<sup>1,5,11</sup> Detailed magnetization measurements have been carried out to characterize this spin-ordering phenomenon in the present chain polymorph.

## Experimental Section

**$[\text{Mn}(\text{salpn})\text{NCS}]_2$ .** In a beaker open to the atmosphere, 229 mg (1.88 mmol) of salicylaldehyde and 71 mg (0.96 mmol) of 1,3-diaminopropane were stirred into 40 mL of ethanol.  $\text{Mn}(\text{CH}_3\text{CO}_2)_2 \cdot 4\text{H}_2\text{O}$  in an amount of 245 mg (1.00 mmol) was added, and the stirring continued for about 1 h. To the resulting solution, 200 mg (2.06 mmol) of KNCS dissolved in a minimum amount of water was added. The solution was allowed to stand for about 3 h to complete the air oxidation of Mn(II). The filtered solution was then kept aside at room temperature ( $\sim 35^\circ\text{C}$ ) for 2–3 days, over which time dark green crystals deposited. Yield: 330 mg (0.84 mmol, 89%). Anal. Calcd for  $\text{MnC}_{18}\text{H}_{16}\text{N}_3\text{O}_2\text{S}$ : C, 54.96; H, 4.10; N, 10.68. Found: C, 54.48; H, 4.13; N, 10.70. Important IR absorptions ( $\text{cm}^{-1}$ ): 2043, 1601, 1543, 1468, 1443, 1396, 1310, 1148, 1124, 1076, 1030, 977, 895, 804, 754, 613, 463. When the ambient temperature was lower ( $18\text{--}20^\circ\text{C}$ , for example, in winter) the solution affords small amounts of the polymeric form along with the dimer. Recrystallization from acetonitrile gives pure dimer over a wide range of temperatures ( $5\text{--}30^\circ\text{C}$ ).

**$[\text{Mn}(\text{salpn})\text{NCS}]_n$ .** The procedure is the same as that for the dimer described above, except that the final solution was kept in a refrigerator ( $5^\circ\text{C}$ ) for 8–10 days. The yield of dark green crystals of the polymer in a typical experiment was 85%. Anal. Calcd for  $\text{MnC}_{18}\text{H}_{16}\text{N}_3\text{O}_2\text{S}$ : C, 54.96; H, 4.10; N, 10.68. Found: C, 54.63; H, 4.38; N, 10.65. Important IR absorptions ( $\text{cm}^{-1}$ ): 2068, 1609, 1541, 1466, 1400, 1300, 1150, 1126, 1067, 1028, 968, 903, 804, 750, 615, 459.

**Polymorphism.** To study the effect of solvent, the dimer obtained from the reaction in ethanol at  $35^\circ\text{C}$  was recrystallized from various solvents, viz., acetonitrile, dichloromethane, acetone, tetrahydrofuran, methanol, and ethanol. In each case, crystallizations were done at two temperatures, viz.,  $35$  and  $5^\circ\text{C}$ . The crystalline products obtained after 8–10 days were identified as dimer, polymer, or a mixture of the two by IR spectroscopy (vide supra).

**X-ray Crystallography.** X-ray data were collected for the two polymorphs on an Enraf-Nonius CAD4 diffractometer at room temperature using graphite monochromated  $\text{Mo K}\alpha$  radiation. The structures were solved by a combination of heavy atom and direct methods with SHELX-86<sup>12</sup> and refined with SHELXL-93/SHELXL-97.<sup>13</sup> The polymer was refined as a racemic twin. Crystal data are in Table 1, and selected bond distances and angles are given in

**Table 1.** Crystallographic Data for the Two Polymorphs of  $\text{Mn}(\text{salpn})\text{NCS}$

|                       | dimer  | polymer  |
|-----------------------|--|--|
| formula               | $\text{C}_{18}\text{H}_{16}\text{MnN}_3\text{O}_2\text{S}$ | $\text{C}_{18}\text{H}_{16}\text{MnN}_3\text{O}_2\text{S}$ |
| fw                    | 393.34   | 393.34   |
| <i>A</i>              | 12.573(3) Å  | 12.5277(14) Å  |
| <i>B</i>              | 13.970(7) Å  | 11.576(2) Å  |
| <i>C</i>              | 18.891(9) Å  | 11.513(2) Å  |
| <i>V</i>              | 3318(2) Å <sup>3</sup>                                     | 1669.6(4) Å <sup>3</sup>                                   |
| <i>Z</i>              | 8  | 4  |
| space group           | Pbca   | <i>Pna</i> 2 <sub>1</sub>                                  |
| <i>T</i>              | 293(2) K   | 293(2) K   |
| $\lambda$             | 0.710 73 Å   | 0.710 73 Å   |
| $\rho_{\text{calcd}}$ | 1.575 g cm <sup>-3</sup>                                   | 1.565 g cm <sup>-3</sup>                                   |
| $\mu$                 | 9.38 cm <sup>-1</sup>                                      | 9.33 cm <sup>-1</sup>                                      |
| $R(F_o^2)^a$          | 0.0523   | 0.0219   |
| $R_w(F_o^2)^b$        | 0.1303   | 0.0563   |

<sup>a</sup>  $R = \Sigma |F_o| - |F_c| / \Sigma |F_o|$ . <sup>b</sup>  $R_w = [\Sigma w(F_o^2 - F_c^2)^2 / \Sigma (wF_o^4)]^{1/2} w^{-1} = [\sigma(F_o^2) + (AP)^2 + BP]$ , with  $A = 0.0912$  and  $B = 0.00$  for dimer and  $A = 0.0411$  and  $B = 0.15$  for polymer.  $P = [2F_c^2 + \text{Max}(F_o^2, 0)] / 3$ .

**Table 2.** Selected Bond Lengths (Å) and Angles (deg)<sup>a</sup>

| Dimer Bond Distances   |            |                   |            |
|------------------------|------------|-------------------|------------|
| Mn–O(1)                | 1.844(3)   | Mn–O(2)           | 1.923(3)   |
| Mn–N(1)                | 2.024(4)   | Mn–N(2)           | 2.025(4)   |
| Mn–N(3)                | 2.154(5)   | Mn–O(2)#1         | 2.539(3)   |
| Dimer Bond Angles      |            |                   |            |
| O(1)–Mn–O(2)           | 88.22(13)  | O(1)–Mn–N(1)      | 91.47(15)  |
| O(2)–Mn–N(1)           | 168.77(14) | O(1)–Mn–N(2)      | 173.67(14) |
| O(2)–Mn–N(2)           | 87.31(14)  | N(1)–Mn–N(2)      | 92.04(15)  |
| O(1)–Mn–N(3)           | 95.82(16)  | O(2)–Mn–N(3)      | 99.58(15)  |
| N(1)–Mn–N(3)           | 91.61(16)  | N(2)–Mn–N(3)      | 89.35(16)  |
| O(1)–Mn–O(2)#1         | 92.33(12)  | O(2)–Mn–O(2)#1    | 80.01(12)  |
| N(1)–Mn–O(2)#1         | 88.79(12)  | N(2)–Mn–O(2)#1    | 82.48(13)  |
| N(3)–Mn–O(2)#1         | 171.83(14) |                   |            |
| Polymer Bond Distances |            |                   |            |
| Mn(1)–O(1)             | 1.880(2)   | Mn(1)–O(2)        | 1.897(2)   |
| Mn(1)–N(2)             | 2.037(2)   | Mn(1)–N(1)        | 2.042(2)   |
| Mn(1)–N(3)             | 2.270(3)   | Mn(1)–S(1)#1      | 2.7737(11) |
| Polymer Bond Angles    |            |                   |            |
| O(1)–Mn(1)–O(2)        | 85.37(9)   | O(1)–Mn(1)–N(2)   | 173.20(8)  |
| O(2)–Mn(1)–N(2)        | 88.83(9)   | O(1)–Mn(1)–N(1)   | 90.70(9)   |
| O(2)–Mn(1)–N(1)        | 176.06(8)  | N(2)–Mn(1)–N(1)   | 95.10(9)   |
| O(1)–Mn(1)–N(3)        | 92.63(11)  | O(2)–Mn(1)–N(3)   | 95.13(10)  |
| N(2)–Mn(1)–N(3)        | 91.43(10)  | N(1)–Mn(1)–N(3)   | 84.84(10)  |
| O(1)–Mn(1)–S(1)#1      | 90.47(9)   | O(2)–Mn(1)–S(1)#1 | 95.80(8)   |
| N(2)–Mn(1)–S(1)#1      | 86.57(8)   | N(1)–Mn(1)–S(1)#1 | 84.41(7)   |
| N(3)–Mn(1)–S(1)#1      | 168.84(7)  |                   |            |

<sup>a</sup> Symmetry transformations used to generate equivalent atoms: #1  $-x, -y + 1, -z$  for dimer and  $-x, -y, z + 1/2$  for polymer.

Table 2. Powder diffractograms were measured on a model PW3710 Philips Analytical X-ray diffractometer.

**Optical Spectroscopy.** IR spectra were obtained with a Shimadzu FT-IR 8000 spectrometer. Reflectance spectra of powder samples were measured by using a Shimadzu UV-3100 spectrometer equipped with an ISR-3100 integrating sphere attachment.

**Magnetic Measurements.** The two polymorphs obtained from the reaction in ethanol were used for magnetic measurements. The purity of the polymorphs used for magnetic studies were checked by using IR and by comparing their X-ray powder diffraction patterns with those calculated<sup>14</sup> based on crystal structure. The samples were ground and pressed into pellets to avoid orientation effects. Magnetic data were recorded on a MPMS5 magnetometer (Quantum Design Inc.). The calibration was made at 298 K by using a palladium reference sample furnished by Quantum Design Inc.

(14) Kraus, W.; Nolze, G. Powder Cell for Windows version 2.3; Federal Institute for Materials Research and Testing, Berlin: Germany, 1999.

- (7) Miyasaka, H.; Clérac, R.; Ishii, T.; Chang, H.-C.; Kitagawa, S.; Yamashita, M. *J. Chem. Soc., Dalton Trans.* **2002**, 1528.
- (8) Li, H.; Zhong, Z. J.; Duan, C.-Y.; You, X.-Z.; Mak, T. C. W.; Wu, B. *Inorg. Chim. Acta* **1998**, 271, 99.
- (9) Stults, B. R.; Marianelli, R. S.; Day, V. W. *Inorg. Chem.* **1975**, 14, 722.
- (10) Stults, B. R.; Day, R. O.; Marianelli, R. S.; Day, V. W. *Inorg. Chem.* **1979**, 18, 1847.
- (11) Gregson, A. K.; Moxon, N. T. *Inorg. Chem.* **1982**, 21, 586.
- (12) Sheldrick, G. M. SHELXS-86. *Acta Crystallogr.* **1990**, A46, 467.
- (13) Sheldrick, G. M. SHELXL-93; University of Göttingen: Germany, 1993; SHELXL-97; University of Göttingen: Germany, 1997.

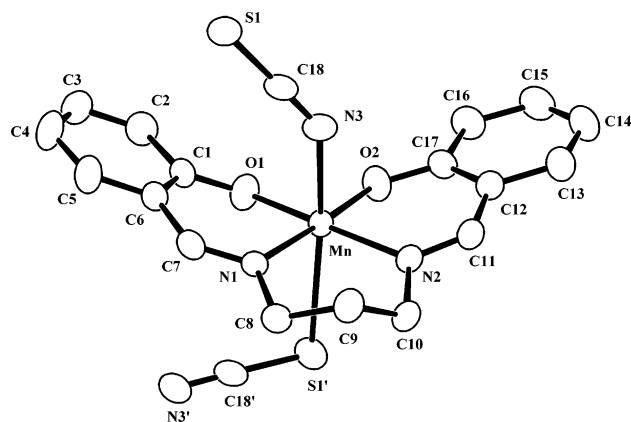


**Figure 1.** ORTEP view of one complex cation and its two bonded thiocyanate anions along the 1D chains of  $[\text{Mn}(\text{salpn})\text{NCS}]_n$  in polymer. Hydrogen atoms are omitted for clarity, and the thermal ellipsoids are represented at 50% probability level.  $' = -x, -y, z + 1/2$

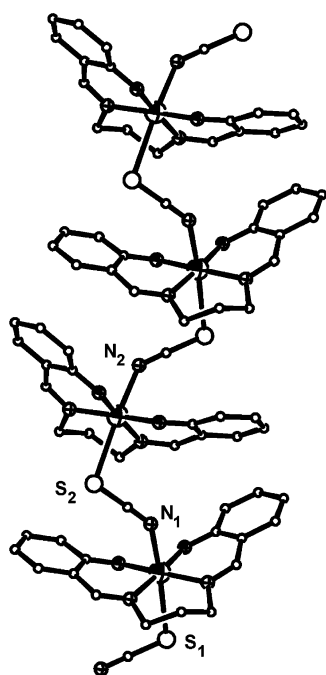


**Figure 2.** Perspective view of helical chains in the polymer. Atom codes: Large shaded spheres, Mn; small shaded spheres, O; small footballs, N; large open circles, S; small open circles, C. The labels pertain to the discussion on canting geometry.

The magnetic susceptibility data were collected over a temperature range of 2–300 K at a magnetic field of 2000 G for  $[\text{Mn}(\text{salpn})\text{NCS}]_n$  and 500 G for  $[\text{Mn}(\text{salpn})\text{NCS}]_2$  and were corrected for diamagnetism using Pascal's constants. In the case of  $[\text{Mn}(\text{salpn})\text{NCS}]_n$ , the  $\chi_M T$  versus  $T$  curve was fitted, in the range 15–300 K, by using the classical  $S = 2$  chain law,<sup>15</sup> based on the Heisenberg model.

## Results and Discussion

**Structure of  $[\text{Mn}(\text{salpn})\text{NCS}]_n$ .** The structure of the polymer (Figures 1 and 2) is analogous to that of the azide complex.<sup>1</sup> The salpn binds in the equatorial mode and

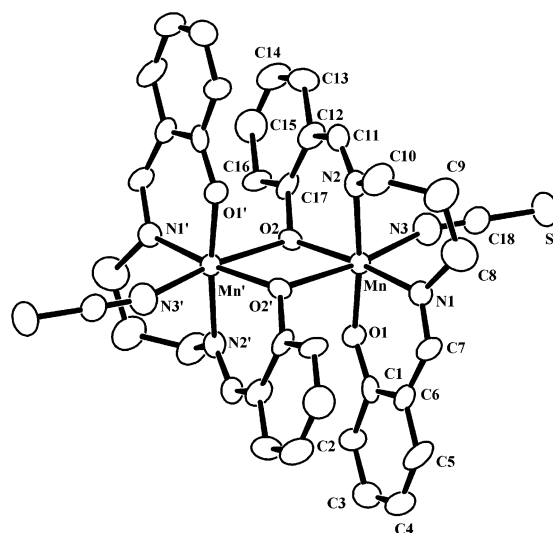


**Figure 3.** ORTEP view of the  $\text{Mn}(\text{salpn})\text{NCS}$  dinuclear complex molecule in the dimer. Hydrogen atoms are omitted for clarity, and the thermal ellipsoids are represented at the 50% probability level.  $' = -x, -y + 1, -z$

thiocyanate acts as an end-to-end bridge. Each monomeric unit is related to its adjacent ones by a 2-fold screw axis, leading to a helix propagating along the crystallographic  $c$ -axis. While the gross structure is similar to that of the azide, there are significant differences in the coordination geometry. The two in-plane Mn–N distances in the azide complex were unequal, which was attributed to the strain involved in the spiral formation. In contrast, the thiocyanate has equal in-plane Mn–N distances. The long Mn–S bond apparently relieves any strain in the polymer chain formation. The Jahn–Teller axis of Mn(III) corresponds approximately to the N3–Mn–S direction. We will see later the impact of this distortion on the magnetic properties. The inclination between the mean planes of the two halves of the SB ligand (excluding the methylene groups) is now  $37.2(1)^\circ$  as opposed to  $44.0(1)^\circ$  in the azide complex.

Besides the previously mentioned azide bridged complexes,<sup>1,8–10</sup> several other polymeric chain compounds of Mn(III), most of them containing acetate bridges, are known.<sup>16–20</sup> The unique feature of the chains in  $\text{Mn}(\text{salpn})\text{N}_3$  and  $\text{Mn}(\text{salpn})\text{NCS}$  is that the adjacent repeat units are related by a crystallographic screw axis leading to a helical chain crystallizing in a chiral space group.

**Structure of  $[\text{Mn}(\text{salpn})\text{NCS}]_2$ .** In the dimer also (Figure 3) the salpn ligands adopt the equatorial coordination mode; however, the two halves of each salpn are now more coplanar than in the helical chain, the interplanar angle being  $10.2(1)^\circ$ . The thiocyanate ions remain terminal and N-bonded. Six coordination around the manganese atoms is completed by two highly unsymmetrical (Mn–O 1.923(3), 2.539(3) Å)

(15) Fisher, M. E. *Am. J. Phys.* **1964**, *32*, 343. The Hamiltonian, in zero-field, is of the form  $H = -J\sum_i S_{i+1}$ . The anisotropic terms are not included as they do not significantly influence the magnetic susceptibility above 15 K.

(16) Aurangzeb, N.; Hulme, C. E.; McAuliffe, C. A.; Pritchard, R. G.; Watkinson, M.; Gracia-Deibe, A.; Bermejo, M. R.; Sousa, A. *J. Chem. Soc., Chem. Commun.* **1992**, 1524.  
(17) Davies, J. E.; Gatehouse, B. M.; Murray, K. S. *J. Chem. Soc., Dalton Trans.* **1973**, 2523.  
(18) Akhtar, F.; Drew, M. G. B. *Acta Crystallogr.* **1982**, *B38*, 612.  
(19) Bonadies, J. A.; Kirk, M. L.; Lah, M. S.; Kessissoglou, D. P.; Hatfield, W. E.; Pecoraro, V. L. *Inorg. Chem.* **1989**, *28*, 2037.  
(20) Kirk, M. L.; Lah, M. S.; Raptopoulou, C.; Kessissoglou, D. P.; Hatfield, W. E.; Pecoraro, V. L. *Inorg. Chem.* **1991**, *30*, 2037.

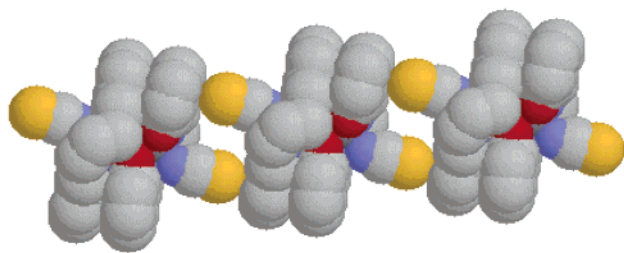


**Figure 4.** RASMOL drawing of 1D chain of dimers linked by S...ring interaction along the  $a$ -axis. Color code for atoms: blue, N; red, O; yellow, S; gray, C; Mn atoms are hidden.

phenoxide bridges. The two halves of the dimer are related by a crystallographic inversion center.  $\text{SCN}-\text{Mn}-\text{O}_{\text{bridge}}$  appears to be the Jahn–Teller elongation axis, even though the terminal thiocyanate ion is more strongly bound compared to the bridging thiocyanate in the polymer. The bridge angle  $\text{Mn}-\text{O}_{\text{bridge}}-\text{Mn}'$  is  $100.00(11)^\circ$ , while the  $\text{Mn}-\text{Mn}'$  distance is  $3.4406(11) \text{ \AA}$ . The plane defining the  $\text{MnO}_2\text{Mn}'\text{O}_2'$  bridge makes an angle of  $85.0(1)^\circ$  with the equatorial coordination plane defined by the atoms Mn, N1, N2, O1, and O2.

The uncoordinated S has a significant role in stabilizing the crystal structure. The most remarkable feature is the  $\text{S}-\pi$  (phenyl) interactions which connect the dimers into one-dimensional chains running along the crystallographic  $a$ -axis (Figure 4). The distance between the S atom and the centroid of the phenyl ring is  $3.66 \text{ \AA}$ , while the C–centroid–S angle is  $90 \pm 11^\circ$  for the six ring C atoms. A search in the Cambridge Crystallographic Database for metal complexes having N-coordinated  $\text{NCS}^-$  ion interacting with the  $\pi$ -cloud of phenyl rings resulted in 57 hits. Restricting the C–centroid–S angle to  $90 \pm 2^\circ$  reduces the number of structures to 14. As expected, the  $\text{S}-\pi$  (phenyl) interaction is a “soft bond”, being influenced by other crystal packing considerations. The four symmetry-related chains are linked into a three-dimensional network through the  $\text{C}-\text{H}\cdots\text{S}$  interaction, the  $\text{S}\cdots\text{H}$  distance being in the range  $3.0\text{--}3.4 \text{ \AA}$ . The bridging through the phenolate oxygen brings the phenyl rings on the two halves of the dimer into close proximity, resulting in four  $\text{C}\cdots\text{C}$  contacts, on each side, in the range  $3.37\text{--}3.50 \text{ \AA}$ . By contrast, the coordination in  $\text{Mn}(\text{salen})\text{NCS}$  has been described as essentially a five-coordinate square pyramidal,<sup>6</sup> with a rather long  $\text{Mn}-\text{O}_{\text{bridge}}$  distance of  $2.750 \text{ \AA}$ .<sup>7</sup> It has been generally observed that the most symmetrical bridge geometry results when water is the axial ligand.<sup>7</sup> Thiocyanate and chloride ligands were found to produce much weaker interaction with the bridging oxygen atom. The present structure is an exception, since the  $\text{Mn}-\text{O}_{\text{bridge}}$  distance is comparable to that in the aquo complexes.

**Polymorphism and Optical Spectra.** Crystallization leads to one or the other polymorph or a mixture of the two depending upon the solvent and temperature. Acetonitrile and dichloromethane give only the dimer at both room temperature,  $35^\circ\text{C}$  (RT), and low temperature,  $5^\circ\text{C}$  (LT). The situation is similar in tetrahydrofuran, except that a small amount of polymer is also obtained at RT along with the dimer. Acetone produces a mixture at both temperatures, the

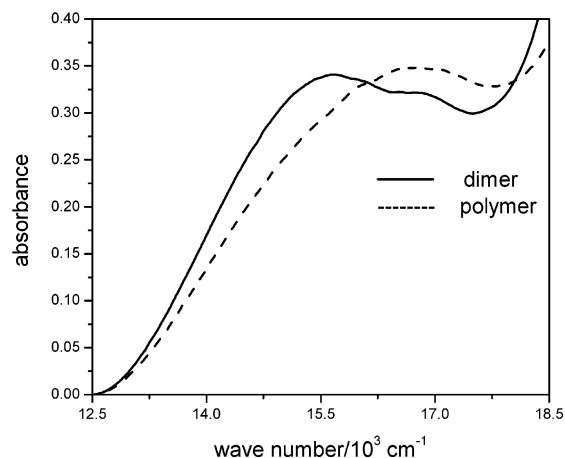


**Figure 5.** Powder diffuse reflectance spectra of polymeric and dimeric  $\text{Mn}(\text{salpn})\text{NCS}$ .

amount of polymer being more at LT. Both methanol and ethanol give the dimer at RT and the polymer at LT. In the case of ethanol the LT product is contaminated with a small amount of the dimer. It turns out that the dimer is the preferred form at RT in all solvents studied. Pure polymer is obtained only from methanol at LT. It is to be noted that even after complete evaporation of the solvent, there is no noticeable amount of dimer in the product obtained at LT from methanol, implying that dimer is kinetically not favored at this temperature in this solvent. The two polymorphs can be readily distinguished based on the IR absorption frequency corresponding to the N–C stretching vibration of the thiocyanate ion:  $2043 \text{ cm}^{-1}$  dimer;  $2068 \text{ cm}^{-1}$  polymer. The rest of the IR region ( $3000\text{--}400 \text{ cm}^{-1}$ ) is virtually identical for the two compounds. This is consistent with the general observation that the N-bonded thiocyanate ions have a lower N–C stretching frequency than the bridging thiocyanate.<sup>21</sup>

The different coordination environments in the two compounds is also reflected in the  $d-d$  absorption region: band maxima at  $15\,690$  and  $16\,710 \text{ cm}^{-1}$  for dimer,  $16\,750 \text{ cm}^{-1}$  for polymer (Figure 5). The solution spectra in acetonitrile has several features and agree closely with the previously reported spectrum in aqueous solution:<sup>3</sup>  $16\,750$  (220),  $21\,100$  (1200),  $25\,640$  (5000),  $36\,100$  ( $17\,600 \text{ cm}^{-1}$  ( $\text{L mol}^{-1} \text{ cm}^{-1}$ )). The species present in solution is, in all probability, solvent perturbed  $\text{Mn}(\text{salpn})\text{NCS}$ . The bands at  $21\,100$  and  $25\,640 \text{ cm}^{-1}$  are probably due to ligand-to-metal charge-transfer transition. The weak band at  $16\,750 \text{ cm}^{-1}$  is assigned to  $d-d$  transitions and may include in its envelope the transitions from the split components of the  $^5\text{E}$  state. The splitting is more prominent in the reflectance spectrum of the dimer, which has only a weak axial interaction with the phenolate oxygen atoms.

**Magnetic Properties.** Magnetic susceptibility of the chain compound  $[\text{Mn}(\text{salpn})(\text{NCS})]_n$  was measured between  $300$  and  $2 \text{ K}$ . The results are represented in Figure 6 as the product  $\chi_{\text{M}}T$  per Mn as a function of  $T$ . At  $300 \text{ K}$ ,  $\chi_{\text{M}}T = 2.82 \text{ cm}^3 \text{ mol}^{-1} \text{ K}$ . By itself, this value, which is lower than

(21) Nakamoto, K. *Infrared and Raman Spectra of Inorganic and Coordination Compounds*, 3rd ed.; John Wiley & Sons: New York, 1977; p 270.



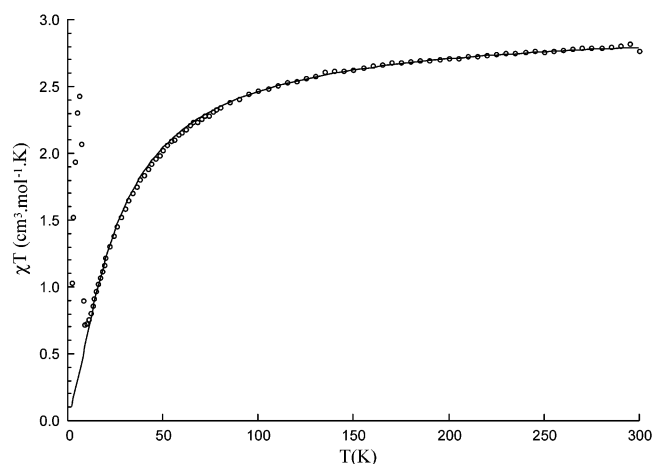


**Figure 6.** Product of the magnetic susceptibility per mole of manganese and temperature for the chain compound  $[\text{Mn}(\text{salpn})\text{NCS}]_n$  (dotted line). Solid line corresponds to the classical spin  $S = 2$  chain model with  $g = 1.99$ ,  $J = -3.2 \text{ cm}^{-1}$  using data above 15 K.

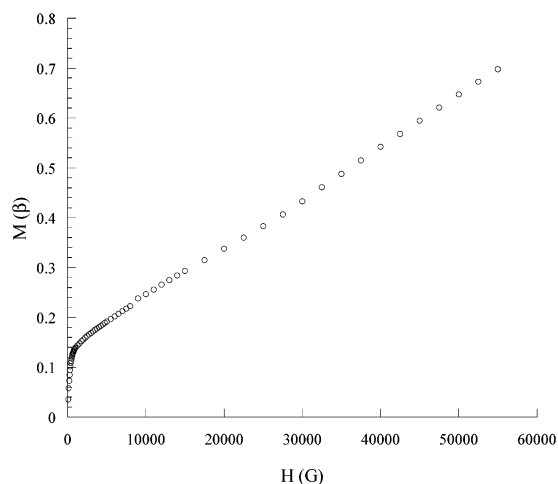


**Figure 7.** Magnetization per mole of manganese for the chain compound  $[\text{Mn}(\text{salpn})\text{NCS}]_n$  as a function of magnetic field.

that for one isolated high spin Mn(III), indicates the presence of an antiferromagnetic coupling in the chain. This is confirmed by the decrease of  $\chi_{\text{M}}T$  as  $T$  decreases. At low temperature, an anomaly is observed in  $\chi_{\text{M}}T$  (see below). The data above 15 K are well-fitted by the law for a chain of classical spins  $S = 2$  with  $J = -3.2 \text{ cm}^{-1}$  and  $g = 1.99$ .

The anomaly in  $\chi_{\text{M}}T$  was found in fact to be related to a spin ordering phenomenon. First, when we recorded the magnetization at 2 K versus magnetic field, we obtained a curve (Figure 7) exhibiting two regimes. At low field, magnetization increases steeply with magnetic field; at higher field magnetization increases at a slower rate and in an almost linear fashion. This is strongly reminiscent of weak ferromagnetism.<sup>22,23</sup> An hysteresis (Figure 8) was detected in the ordered phase at 2 K with a coercive field of 2500 Oe.

The phenomenology of the spin ordering was explored in detail (Figure 9) by measuring the zero field cooled (ZFC)

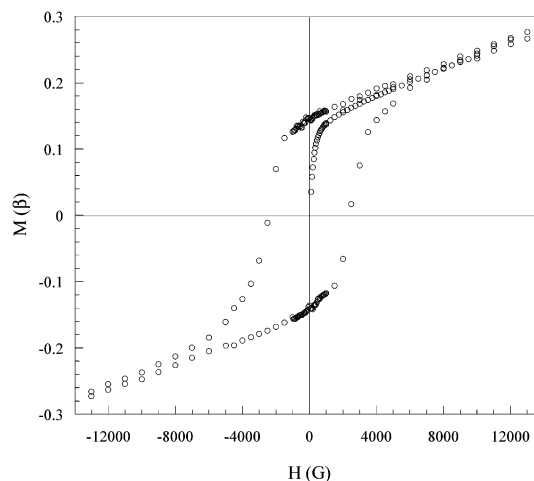


**Figure 8.** Hysteresis in the ordered phase of the chain compound  $[\text{Mn}(\text{salpn})\text{NCS}]_n$  at 2 K.

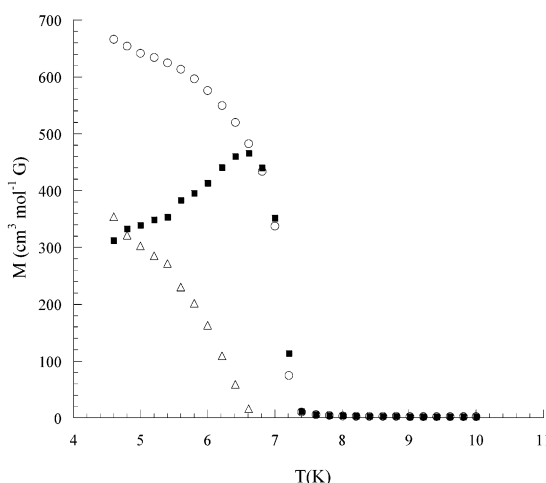


**Figure 9.** Temperature dependence of the magnetization per mole of manganese for the chain compound  $[\text{Mn}(\text{salpn})\text{NCS}]_n$  within a field of 30 G: (■) ZFC; (○) FC. The remnant magnetization was calculated as FC – ZFC (Δ).

and field cooled (FC) magnetization. The sample was cooled under zero field down to 4.5 K; at this temperature the field was set to 30 G and  $T$  was increased to 10 K. The sample was then cooled again under 30 G down to 4.5 K to get FC magnetization. As expected the FC curve is above the ZFC curve. The difference is indicative of the remnant magnetization, which is found to vanish at  $T_c = 6.8 \text{ K}$ . It has to be noted that the saturation magnetization is only a fraction of the magnetization of a high-spin Mn(III) ( $4\beta$ ), as expected for weak ferromagnetism.

Magnetic susceptibility of  $[\text{Mn}(\text{salpn})(\text{NCS})]_2$  was measured between 300 and 2 K. The results are represented in Figure 10 as the product  $\chi_{\text{M}}T$  as a function of  $T$ . At 300 K the product  $\chi_{\text{M}}T$  was found to be equal to  $6.01 \text{ cm}^3 \text{ mol}^{-1} \text{ K}$ , corresponding to the expected value for two isolated high-spin Mn(III)s. No exchange coupling is detected from these data, the drop in  $\chi_{\text{M}}T$  below  $\sim 5 \text{ K}$  being due to zero field splitting. This is to be contrasted with the situation in the salen series,<sup>7</sup> where it was observed that (i) in  $\text{Mn}^{\text{III}}_2(\text{SB})_2\text{X}_2$ , when  $\text{X} = \text{NCS}^-$  or  $\text{Cl}^-$ , the trans  $\text{Mn}-\text{O}_{\text{bridge}}$  is long ( $3.44-3.76 \text{ \AA}$ ), whereas when  $\text{X} = \text{OH}_2$ , it is short ( $2.43-2.66 \text{ \AA}$ ), and (ii) short bridges result in stronger ferromagnetic

(22) Carlin, R. L.; Van Duyneveldt, A. J. *Magnetic properties of Transition Metal Compounds*; Springer-Verlag, Inc.: New York, 1977; Vol. 2, p 184.

(23) Bakalbassis, E.; Bergerat, P.; Kahn, O.; Jeannin, S.; Jeannin, Y.; Dromzee, Y.; Guillot, M. *Inorg. Chem.* **1992**, *31*, 625.

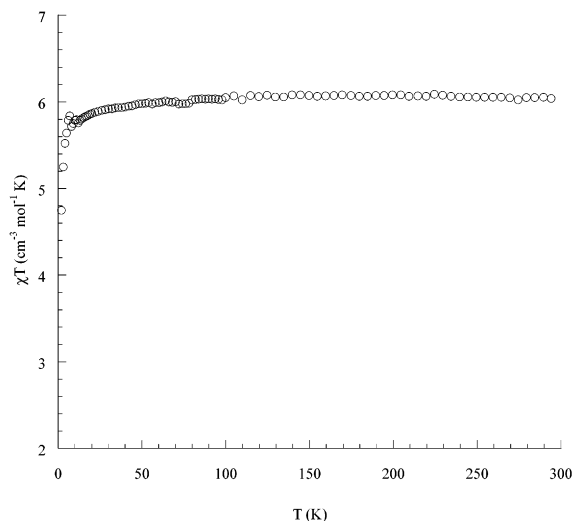


**Figure 10.** Product of the magnetic susceptibility per mole of manganese and temperature for the dimer compound  $[\text{Mn}(\text{salpn})\text{NCS}]_2$ .

interaction ( $J \sim 3.0 \text{ cm}^{-1}$ ). In  $\text{Mn}_2(\text{salpn})_2(\text{NCS})_2$ , the  $\text{Mn}-\text{O}_{\text{bridge}}$  is short, but  $J \sim 0$ . There is no doubt that the  $\text{Mn}-\text{O}_{\text{bridge}}$  distance in the observed range is to some extent influenced by crystal packing considerations. However, the disagreement of the present dimer with the observed magneto-structural correlation in the salen series is more difficult to explain.

**Origin of the Weak Ferromagnetism of the Chain Compound.** The antiferromagnetic nature of the  $\text{NCS}^-$ -mediated coupling in the chain compound is quite clear from above. It is also well-known that  $\text{Mn}(\text{III})$  complexes exhibit a large anisotropy (typically  $D = -4 \text{ cm}^{-1}$  for an elongation).<sup>24,25</sup> From the crystal structure, it was observed that the  $\text{Mn}(\text{III})$  ions are in an elongated environment with the Jahn–Teller (JT) elongation axis oriented toward the  $\text{NCS}^-$  anion. The fourth unpaired electron is then in a  $d_z^2$  orbital with the  $z$ -axis along the JT axis. As a consequence the axial anisotropy energy component must be negative, which means the spins will tend to orient along the JT axis.<sup>25</sup>

It has to be remarked that the JT axis is tilted relative to the chain axis by  $23^\circ$  if we take the  $\text{Mn}_n\text{Mn}_{n+2}\text{S}_n$  angle and by  $34^\circ$  if we take  $\text{Mn}_n\text{Mn}_{n+2}\text{N}_n$  angle. Let us calculate the canting angle, i.e., the angle between two successive spins  $S_1$  and  $S_2$  along the chain. We will assume that  $S_1$  and  $S_2$  are along the respective bisecting vectors. We define

$$\vec{u} = 0.5(\overrightarrow{\text{Mn}_1\text{S}_1} + \overrightarrow{\text{N}_1\text{Mn}_1})$$

$$\vec{v} = 0.5(\overrightarrow{\text{Mn}_2\text{S}_2} + \overrightarrow{\text{N}_2\text{Mn}_2})$$

where  $S_1$ ,  $\text{Mn}_1$ ,  $\text{N}_1$  and  $S_2$ ,  $\text{Mn}_2$ ,  $\text{N}_2$  belong to adjacent (screw related) units in Figure 2.

From the X-ray structure we determined

$$(\vec{u}, \vec{v}) = 55^\circ$$

As a consequence, the uncompensated moment per Mn can be estimated as

$$M_s = M_0 \sin[(\vec{u}, \vec{v})/2] = 4\beta \sin(55/2) = 1.84\beta$$

This is almost 10 times larger than the saturation moment, which can be estimated from measurements at 2 K (Figure 7). We assume that the low value observed is due to a combination of antiferromagnetic coupling between chains with a canting effect. This would need further studies to be ascertained.

Long-range ordering characterized by an anomalous rise in susceptibility at low-temperatures has been observed also in some other antiferromagnetically coupled  $\text{Mn}(\text{III})$  chain compounds, viz,  $\text{Mn}(\text{acac})_2\text{X}$  ( $\text{X} = \text{N}_3^-$ ,  $\text{NCS}^-$ ),<sup>11</sup>  $\text{Mn}(\text{acen})\text{N}_3$ ,<sup>5</sup> and  $\text{Mn}(\text{salpn})\text{N}_3$ <sup>1</sup> ( $\text{acacH} = \text{acetylacetone}$ ,  $\text{acenH}_2 = \text{N,N'-ethylenebis(acetylacetone imine)}$ ). As explained by Gregson and Moxon,<sup>11</sup> the magnetic ordering requires a negative zero field splitting, which is guaranteed by the tetragonally elongated coordination of  $\text{Mn}(\text{III})$  in all the above chain compounds.

## Conclusion

Two factors related to the formation of helical chain are the flexibility of the  $\text{salpn}$  ligand, which allows considerable deviation from coplanarity of the two halves of this ligand (inclination angle  $37^\circ$  in the thiocyanate complex,  $44^\circ$  in the azide complex<sup>1</sup>), and the Jahn–Teller elongation along the pseudohalide bridge. In the case of the present thiocyanate complex, a third factor comes into play, viz., the expected low affinity of  $\text{Mn}(\text{III})$  for coordination with S. This factor would contribute to the relative stability of the dimer despite the highly unsymmetrical nature of the phenolate bridges. An important feature of the dimer is the interaction between the phenyl ring and the free S atom of the thiocyanate ion. While such interactions are present in other crystal structures as shown by the database search, the importance of this noncovalent interaction has not yet been fully appreciated. Although the preferred crystallization of the dimer from most solvents is certainly related to the above factors, it is not clear why the polymer is the kinetically preferred product from methanol and ethanol.

The thiocyanate-mediated exchange along the helical chain is weakly antiferromagnetic. However, below 7 K a magnetic ordering with weak ferromagnetic coupling sets in. It is shown that, in the present case, the weak ferromagnetism arises through large magnetic anisotropy in  $\text{Mn}(\text{III})$  and resultant spin-canting with respect to the chain direction. The low value of the observed saturation moment compared to the expected value based on the canting geometry may be due to antiferromagnetic interaction between chains. Since there are no noncovalent bonds between chains, one would speculate that this coupling arises from nonbonded contacts in the lattice and would require more detailed studies in this and other systems. It may be further noted that  $S = 2$  infinite chains are of interest in the context of the Haldane conjecture,<sup>26</sup> experimental verification of which requires single-crystal measurements on 1D chains of integer spin ions.

(24) Barra, A.-L.; Gatteschi, D.; Sessoli, R.; Abbati, G. L.; Cornia, A.; Fabretti, A. C.; Uytterhoeven, M. G. *Angew. Chem., Int. Ed. Engl.* **1997**, *36*, 2329.

(25) Gerritsen, H. J.; Sabisky, E. S. *Phys. Rev.* **1963**, *132*, 1507.

The structure and magnetic properties of the dimer are at variance with the recently observed trends in phenolate-bridged Mn(III) dimers of salen-type Schiff base ligands.<sup>7</sup> The present dimer has a short bridge despite the strong axial ligand (NCS<sup>-</sup>) and magnetic interaction is absent. With regard to structure, while it is reasonable to expect the axial ligand to have the major role in controlling the structure of the dimer that may form in solution (and more definitely in the gas phase), in the crystal lattice the phenolate interaction should not be considered in isolation but should be taken together with other possible noncovalent interactions, especially the S- $\pi$ (phenyl) interaction and stacking interactions.<sup>27</sup> With regard to magnetic coupling, the net exchange parameter has contributions from several exchange pathways

involving the four magnetic orbitals on each  $d^4$  ion and may be influenced by terminal ligands as well as bridge geometry. More phenolate bridged systems need to be studied to establish the correlations.

**Acknowledgment.** This work was supported by CSIR, India.

**Supporting Information Available:** One crystallographic file, in CIF format, is available on the Internet only. Access information is given on any current masthead page.

IC0256617

(26) Haldane, F. D. M. *Phys. Lett.* **1983**, 93A, 464; *Phys. Rev. Lett.* **1983**, 50, 1153.

(27) Several noncovalent interactions, though generally weaker than the coordinate bonds, can sometimes strongly influence the coordination geometry and conformation in crystals. Swarnabala, G.; Rajasekharan, M. V. *Polyhedron* **1996**, 15, 3197. Sailaja, S.; Swarnabala, G.; Rajasekharan, M. V. *Acta Crystallogr.* **2001**, C57, 1162.